Understanding the phase-change mechanism of rewritable optical media

ALEXANDER V. KOLOBOV[1]*†, PAUL FONS[1], ANATOLY I. FRENKEL[2], ALEXEI L. ANKUDINOV[3], JUNJI TOMINAGA[1] AND TOMOYA URUGA[4]

[1]Center for Applied Near-Field Optics Research, National Institute of Advanced Industrial Science and Technology, Tsukuba Central 4, 1-1-1 Higashi, Tsukuba, Ibaraki 305-8562, Japan
[2]Department of Physics, Yeshiva University, 245 Lexington Avenue, New York, New York 10016, USA
[3]Department of Physics, Box 351560, University of Washington, Seattle, Washington 98195, USA
[4]SPring-8, Japan Synchrotron Radiation Research Institute, Mikazuki, Hyogo 679-5198, Japan
*On leave from: A. F. Ioffe Physico-Technical Institute, 26 Polytechnicheskaya St., 194021 St Petersburg, Russia
†e-mail: a.kolobov@aist.go.jp

Published online: 12 September 2004; doi:10.1038/nmat1215

Present-day multimedia strongly rely on rewritable phase-change optical memories. We demonstrate that, different from the current consensus, $Ge_2Sb_2Te_5$, the material of choice in DVD-RAM, does not possess the rocksalt structure but more likely consists of well-defined rigid building blocks that are randomly oriented in space consistent with cubic symmetry. Laser-induced amorphization results in drastic shortening of covalent bonds and a decrease in the mean-square relative displacement, demonstrating a substantial increase in the degree of short-range ordering, in sharp contrast to the amorphization of typical covalently bonded solids. This novel order–disorder transition is due to an umbrella-flip of Ge atoms from an octahedral position into a tetrahedral position without rupture of strong covalent bonds. It is this unique two-state nature of the transformation that ensures fast DVD performance and repeatable switching over ten million cycles.

Recent advances in multimedia would have been impossible without computer performance getting faster and the stored information denser[1]. The ability of media to be used repeatedly, that is, to be rewritable, is also an important requirement. One of the most promising media for rewritable applications is phase-change materials. The idea to use an amorphous-to-crystalline phase transition for information storage dates back to the 1960s when S. R. Ovshinsky suggested a memory switch based on changes in the properties of amorphous and crystalline phases of multicomponent chalcogenides[2]. A landmark was achieved in the late 1980s by Matsushita/Panasonic who developed phase-change optical disc technology that remained stable over a million use cycles[3]. This technology became the mainstream in optical disc production and in the late 1990s resulted in the commercialization of 4.7 GB digital versatile disc random access memory (DVD-RAM). During the development process, various materials were examined, and the best performing in terms of speed and stability were found to be $Ge_2Sb_2Te_5$ (GST) used in DVD-RAM and an AgInSbTe alloy used in DVD-RW (ref. 4).

The phenomenology of phase-change optical recording is simple. An initially amorphous as-deposited GST layer is crystallized by exposure to a laser beam of intensity sufficient to heat the material to a temperature slightly above the glass-transition temperature. A subsequent exposure to an intense and short laser pulse melts the GST that is then converted into the amorphous state on quenching. A recorded bit is an amorphized mark against the crystalline background. The reversibility of the crystallization–amorphization process allows fabrication of rewritable memory.

The stable crystal structure of GST is hexagonal[5] but the structure of a thin laser-crystallized layer is believed to be different[6]. Based on X-ray diffraction (XRD) measurements, it was argued that a crystallized GST layer possessed the rocksalt structure with Te atoms occupying

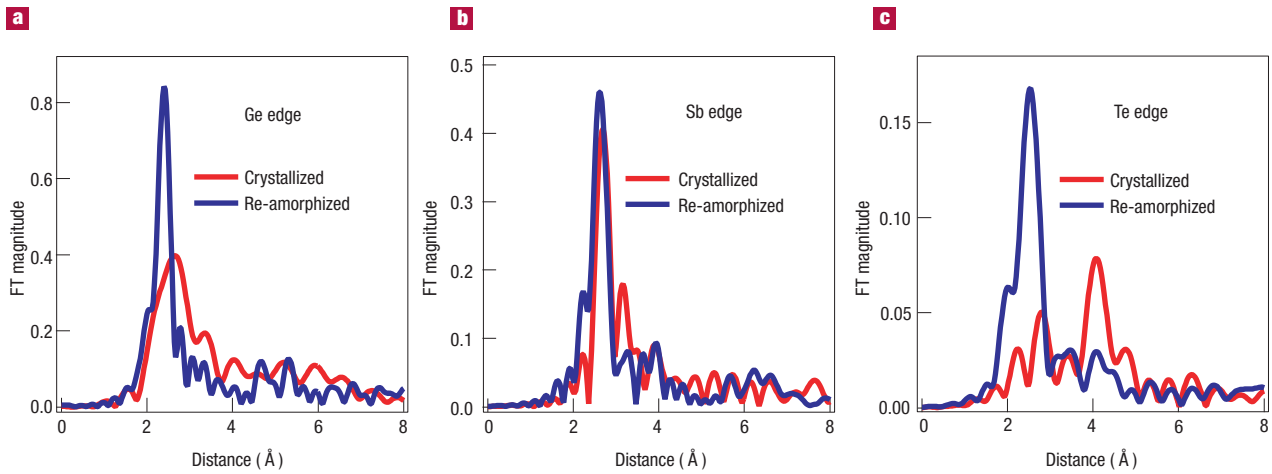

Figure 1 Fourier-transformed EXAFS spectra for crystallized and laser-amorphized samples. Spectra measured at the K-edges of: **a**, Ge, **b**, Sb and **c**, Te. On amorphization the bonds become shorter (as shown by shifts in the peak positions) and stronger, that is, more locally ordered (as shown by increases in the peak amplitudes and concurrent decreases in the peak widths). It should be specially noted that the r-space data shown in the figure are not real-space radial distribution function data but the magnitude of the Fourier transforms (FTs) of the k-space EXAFS data. The peak positions are shifted from the actual interatomic distances towards lower r because of the photoelectron phase shift δ(k) in the phase factor of the EXAFS oscillations. Additionally, contributions from different nearest neighbours interfere producing extra features in the FTs. These effects were properly accounted for during the data analysis.

sites on one face-centred-cubic (f.c.c.) sublattice with Ge and Sb randomly forming the other f.c.c. sublattice (20% of the sites being vacant)[7,8]. A lattice parameter of 6.02 Å was reported. The isotropic atomic displacements found were quite large, especially for the Ge and Sb sites[7,8]. The structure of the amorphous phase has remained unknown and was tacitly assumed to possess a randomized rocksalt structure.

A paradoxical situation exists when a device such as an optical disc is functional and commercially available but the structural changes behind the utilized transition are unknown.

An ideal tool to investigate the local structure of a material and its changes on the atomic scale independent of the state of the material (crystalline or amorphous) is X-ray absorption fine-structure spectroscopy (XAFS)[9].

Raw extended XAFS (EXAFS) oscillations for the crystalline and laser-amorphized samples are shown in the Supplementary Information (Fig. S1). The Fourier-transformed (FT) spectra for the three edges are shown in Fig. 1. A comparison of the experimental and simulated EXAFS is shown in the Supplementary Information (Fig. S2) and the main results are summarized in Table 1.

For the crystalline phase we used the rocksalt structure as the starting structural model for data fitting. By varying the corrections to the ideal rocksalt structure distances, we obtained the following bond lengths: Te–Ge, 2.83 Å; Te–Sb, 2.91 Å (the typical uncertainty in the bond length is ±0.01 Å). No Sb–Ge bonds were detected, which agrees with the fact that Sb and Ge do not intermix in the solid phase. Additionally we observed a second-nearest-neighbour Te–Te peak at 4.26 Å. Unexpectedly, we found that the overall fit intensity was significantly less than predicted, strongly suggesting that the actual coordination number is not six as required by the rocksalt structure but at least a factor of two lower.

It should also be mentioned that whereas the isotropic atomic displacement $\langle u^2 \rangle$ of single atoms obtained from XRD, especially for Ge and Sb species, are quite large (0.04 Å^2), the mean-square relative displacements (MSRD) of the Te–Ge and Te–Sb bond length obtained in EXAFS are considerably lower (0.02 Å^2). This result demonstrates that Ge and Sb atoms deviate from the ideal rocksalt positions not in a random way but in a strongly correlated manner with respect to the neighbouring Te atoms, that is, the crystalline structure is in fact a distorted rocksalt-like structure similar to the case of the ferroelectric GeTe.

The above results suggest the following model. The structure is similar to the rocksalt structure but due to differences in the covalent radii of the constituent species, Ge, and to a lesser extent Sb, are shifted from the corresponding f.c.c. sites, giving rise to a system of shorter bonds and longer bonds in an overall buckled structure[10]. The shorter bonds are more rigid and thus provide a framework for the local structure. It is worth mentioning that a similar mechanism, namely weaker back-bonding to second-nearest neighbours has been argued[11] to be the reason for cohesion between the layers in the rhombohedral structure of IV-VI compounds.

We would like to note that explicit use of a bimodal bond-length distribution where both shorter and longer Ge–Te and Sb–Te bonds were included in the fitting procedure did not influence the results for the shorter bonds. The values obtained for the longer Ge–Te and Sb–Te bonds were around 3.2 Å, that is, longer than in the average periodic structure as expected. The uncertainties were too large to draw more specific conclusions about the longer bonds.

The obtained results are in good agreement with previous XRD measurements. Indeed, in the XRD analysis it was found that the isotropic temperature factor B_0 for Te, and Ge(Sb) species were 1.2 Å^2 and 3.2 Å^2, respectively, which corresponds to atomic displacements of 0.1 Å and 0.2 Å for Te and Ge(Sb) species, respectively. In the analysis used, the atoms are assumed to vibrate independently, therefore the Te–Ge(Sb) bonds thus possess the length of 3.0(1) ± 0.3 Å. This value agrees very well with the values for Ge–Te and Sb–Te bonds obtained from EXAFS analysis, the latter providing much more accurate values. Yet better evidence of the consistency of the two techniques is a comparison of Te–Te distances. The lattice parameter of 6.02 Å obtained from XRD implies a Te–Te distance of 4.26 (± 0.2 Å) which is in excellent agreement with the direct Te–Te distance measurement by EXAFS (4.26 ± 0.01 Å).

It is worth mentioning that the obtained Ge–Te bond length is close to the shorter Ge–Te bond length in the binary GeTe (2.80–2.84 Å)[12,13]

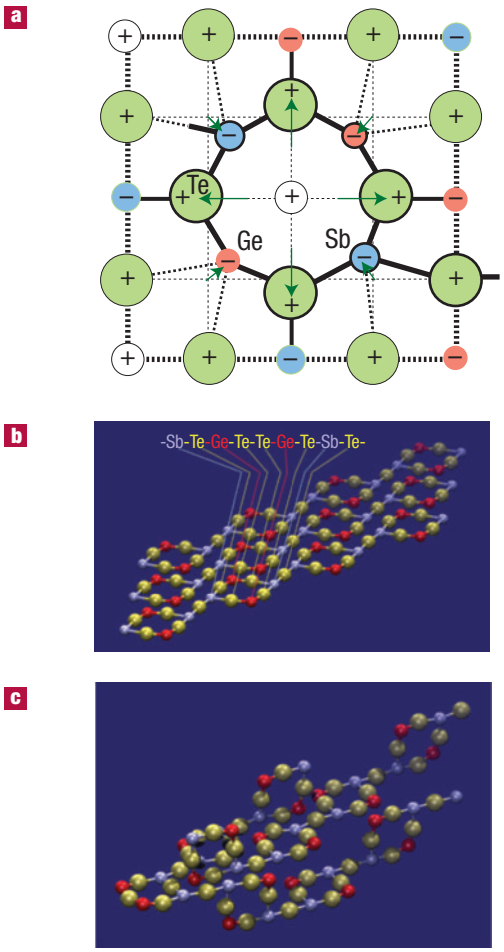

Figure 2 The crystal structure of laser-amorphized GST. a, A schematic two-dimensional image of the lattice distortion of the rocksalt structure due to charge redistribution between the constituent elements; atoms that form the building block of the GST structure are shown using thick lines. The arrows indicate displacements of atoms from the ideal rocksalt positions. **b**, The ideal structure of GST, constructed from the above building blocks; notice that the structure can be viewed as a 'layered' structure consisting of repeated sequences of nine like-atom layers as marked in the figure. **c**, A fragment of the three-dimensional GST structure constructed from rigid building blocks; it should be noted that for the different spatial orientations of the building blocks to be clearly visible, only part of the space has been filled with the building blocks. Notice that although the spatial distribution of Ge and Sb atoms and vacancies is random on a long-range scale, on a short-range scale these entities are parts of rigid building blocks.

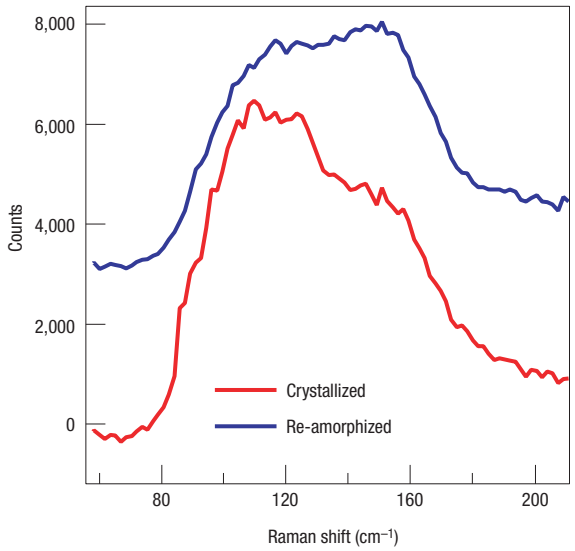

Figure 3 Raman scattering spectra for crystallized and re-amorphized $Ge_2Sb_2Te_5$ layers. The spectra were collected at room temperature using a backscattering geometry; the excitation source was a He-Ne laser (633 nm, 5 mW).

suggesting similar mechanisms for the rocksalt structure distortion in the two materials.

In the ideal rocksalt structure, in order to form six saturated covalent bonds with two electrons per bond, it is necessary for Ge, Sb and Te to possess six valence electrons each. In particular, Ge thus requires two additional electrons whereas each Sb requires one additional electron. These missing electrons must be donated to Ge/Sb and can be exactly provided by orbitals on Te pointing into vacancies. (See Supplementary Information for details.) Although this is a simplified picture, it strongly suggests that vacancies are an intrinsic part of the structure. Consistent with this, experiments in which the concentration of Sb (ref. 8) or Ge (ref. 14) were increased in GST showed that the extra Ge/Sb atoms did not occupy the vacancies, but rather accumulated at grain boundaries or phase segregation took place[8,14].

It should be noted that crystalline GeTe, whose structure at room temperature is distorted rocksalt, inevitably possesses a certain amount of vacancies on Ge sites[15,16], up to 10% in films prepared by thermal crystallization of an amorphous GeTe layer[13]. It has also been argued that the distorted (rhombohedral) structure of GeTe forms as a result of the intrinsic instability of the unsaturated *p*-type bonds present[11].

A well-defined building block shown in thick lines in Fig. 2a can be identified with a block formula of $Ge_2Sb_2Te_5$ and a perfect two-dimensional lattice can be constructed using this building block (Fig. 2b). For simplicity, only shorter bonds are shown in Fig. 2b. Notice that in terms of atomic positions, this structure can be described as a cross-section of a distorted rocksalt structure with vacancies.

The real crystal deviates from the ideal structure in two respects. First, Ge and Sb atoms may swap places producing randomness in the Ge/Sb sublattice. Secondly, each additional building block may rotate by 90 degrees in an arbitrary direction. If one now arbitrarily fills space with these rigid building blocks, the result is a structure in which the Te atoms form an f.c.c. sublattice and Sb and Ge atoms, together with 'vacancies' form the other f.c.c. sublattice. A fragment of such a structure is shown in Fig. 2c. An important point is that whereas Ge, Sb and vacancies are randomly placed on a long-range scale, on a short-range scale they form well-defined rigid building blocks.

It is instructive to notice that the ideal structure shown in Fig. 2b can be viewed as a 'layered' structure of nine like-atom layers with the stacking sequence -Sb-Te-Ge-Te-Te-Ge-Te-Sb-Te-, as marked in Fig. 2b. This sequence is identical to that determined[5] for the stable hexagonal structure of GST. We believe that the formation of the ordered chain structure is a prelude for the phase transformation from the rocksalt-like to hexagonal structure. In our differential scanning calorimetry (DSC) study of GST, we indeed observed an extra exothermic peak not previously reported between those corresponding to the crystallization of the amorphous layer and the transformation into the hexagonal structure[17].

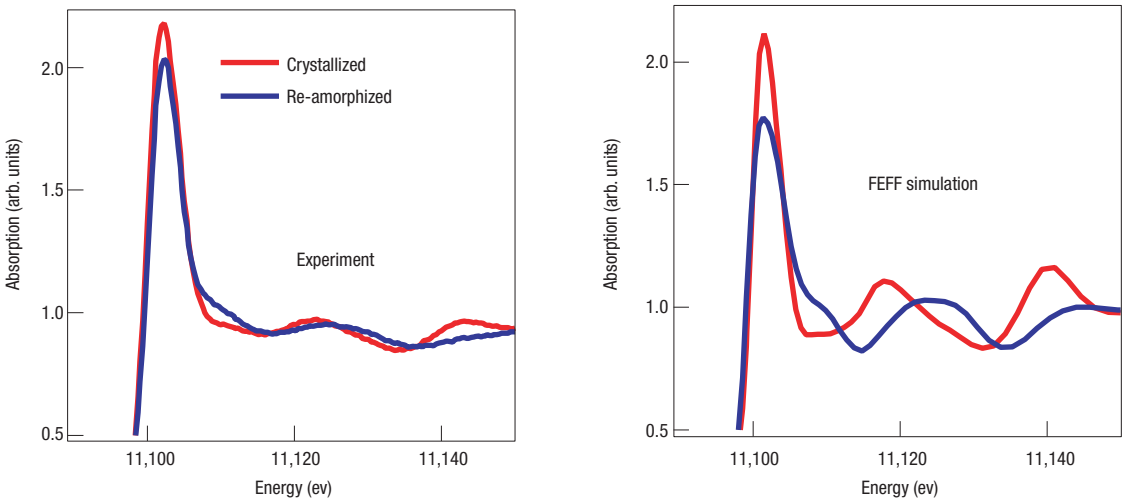

Figure 4 Measured and simulated Ge-edge XANES spectra for GST for the crystalline and amorphous states. Notice that the change in the Ge position from octahedral to tetrahedral coordination perfectly reproduces all the spectral features. The larger amplitudes of the features in the simulation (see Methods) are due to the fact that thermal damping has not been included.

We now turn to the amorphous state. We found that Te–Ge and Te–Sb bonds get shorter (2.61 Å and 2.85 Å, respectively) and stronger as shown by Fig. 1. At the same time, the Te second-neighbour peak becomes considerably weaker but does not disappear completely. The MSRD value decreases from 0.02 Å^2 in the crystalline state to 0.008 Å^2 in the amorphous state. Such behaviour is highly unusual for typical three-dimensional covalently bonded solids, as due to the anharmonicity of interatomic potentials, disordering typically results in an increase of the bond lengths[18]. Interestingly, at the same time the volume of GST has been documented to decrease on crystallization[19]. These seemingly contradictory results remind one of the case of molecular solids where the rupture of intermolecular bonds results in strengthening (shortening) of intramolecular bonds. At the same time, the rupture, or weakening, of the intermolecular interaction also leads to an increase in volume.

These results suggest the following. On melting, inter-block bonds (longer Te–Ge and Te–Sb bonds) are broken and as a result intra-block bonds become shorter and stronger, that is, the amorphous phase is locally more ordered than the crystalline phase. Our Raman scattering experiments provided further grounds for this model, namely, the measured Raman modes for GST (Fig. 3) were more rigid in the amorphous state than in the crystalline state. This situation is similar to the amorphization of Se or Te when interchain interaction is weakened giving rise to a Raman peak located at higher wave number[20].

To get further insight into the structure of the amorphous phase, we performed XANES simulations and found that the best agreement with experiment was obtained when Ge was allowed to acquire its preferred tetrahedral surroundings (Fig. 4). The discrepancy in the amplitudes of the features in the measured and simulated spectra is due to the fact that thermal damping is not included in the simulations.

This structural transformation is illustrated in Fig. 5 and also in Supplementary Information (switch.mov) where a Ge atom is shown within the f.c.c. structure formed by Te atoms. The Ge atoms occupy the octahedral and tetrahedral symmetry positions in the crystalline and amorphous states, respectively. The stronger covalent bonds are shown with thicker lines than the weaker bonds (Fig. 5, left). An intense laser pulse induces rupture of the weaker bonds and the Ge atom flips into the tetrahedral position (Fig. 5, right). An alternative description of the structural transformation on melting is an umbrella-flip distortion resulting in disordering of the Ge sublattice. Notice that the three covalent bonds remain intact. This conservation of the system of stronger covalent bonds is crucial: the material is not molten in a conventional sense.

A check of such a transformation is an estimate of the Ge–Te distance from the crystallographic data. Using a lattice parameter of 6.02 Å (ref. 8), the Ge–Te distance (Ge atoms being in tetrahedral symmetry positions) can be easily calculated to be 2.61 Å, that is, exactly the value obtained from the EXAFS analysis. This consistency between the results obtained using two different structural techniques is the ultimate proof of the suggested structural modification.

The crystallization process is described by a straight line in Arrehnius coordinates with an activation energy of ~2.3 eV (refs 21–23). Such crystallization behaviour is inconsistent with the relaxation of conventional network glasses[24], but follows naturally from the two-state model. We would like to stress that the observed activation energy is significantly larger than the characteristic energy of solid-state processes in GST (whose bandgap is ~0.5 eV) and rather corresponds to a typical bonding energy in molecules.

Although it is generally believed that the role of a laser pulse is to simply heat the material, we argue that electronic excitation creating non-equilibrium charge carriers is crucial for the weakening and subsequent rupture of the subsystem of weaker Ge–Te bonds. Indeed, the presence of longer (weaker) bonds implies that the density of states corresponding to these bonds is lower in energy and hence photogenerated non-equilibrium carriers more readily populate these states making them more susceptible to thermal vibration-induced dissociation. It is speculated here that the presence of the electronic component is critical to the high-speed phase transitions observed in phase-change media.

We would also like to note that in order for the absorbed energy to dissipate non-radiatively, a large number of phonons have to be emitted simultaneously. The presence of states in the bandgap significantly facilitates this process. As a result, heating predominantly occurs in the vicinity of the sites responsible for these states, selectively heating them to a temperature that may considerably exceed the average temperature[25].

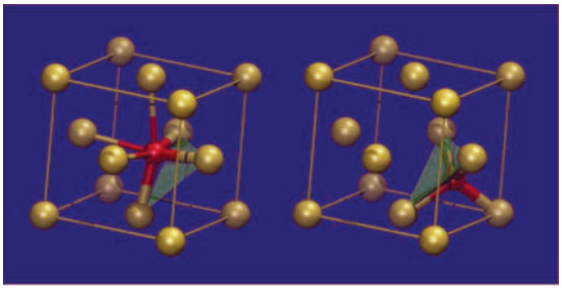

Figure 5 Fragments of the local structure of GST around Ge atoms in the crystalline (left) and amorphous (right) states. Stronger covalent bonds are shown as thicker lines whereas weak interblock bonds are shown as thinner lines. Notice that the stronger covalent bonds remain intact on the umbrella-flip structural transformation rendering the Ge sublattice random. It is this nature of the structural change that makes the medium fast and stable.

Table 1 Comparison of the GST bond lengths determined from EXAFS and XRD analysis for the crystalline and laser-amorphized states.

Bond	Bond length (Å)	
	From EXAFS	From XRD
	Crystallized state	
Ge–Te	2.83 ± 0.01	3.0(1) ± 0.3
Sb–Te	2.91 ± 0.01	3.0(1) ± 0.3
Te–Te (2nd)	4.26 ± 0.01	4.2(6) ± 0.2
	Laser-amorphized state	
Ge–Te	2.61 ± 0.01	2.61*
Sb–Te	2.85 ± 0.01	

*Calculated based on the rocksalt lattice parameter assuming Ge atoms occupy tetrahedrally coordinated sites in the Te f.c.c. sublattice

Structural transformations may thus take place locally without relaxation of the complete structure.

It should be stressed that the above structural transformation involves a change in the hybridization from *p*-type bonding in rocksalt to sp^3-hybridization in the amorphous state. This change in the electronic states accounts for the very large change in optical and electrical properties of GST on the crystallization–amorphization transition. The significant change in electronic structure on the transition is also reflected in the large change observed in the XANES structure—a consequence of the correlated large change in the conduction-band density of states.

Sb-edge XANES does not exhibit any significant changes on amorphization, implying that the local arrangement of atoms around Sb remains essentially unchanged, that is, structural changes 'pivot' around the local arrangement of Sb atoms, which play the role of enhancing overall structural stability. As the spatial extent of the phase transformation is of the order of a lattice constant, the ultimate spatial resolution may be as good as a few ångströms.

To conclude, GST can be viewed as being built from well-defined rigid building blocks of the composition $Ge_2Sb_2Te_5$. In the crystalline state, the constraint on the mutual arrangement of the building blocks in space is such that Te atoms form an f.c.c. lattice. Interblock interaction and long-range ordering cause the resulting structure to resemble the rocksalt structure. In the amorphous state, interblock interaction is weakened, which allows the block structure to relax so that the bonds shrink and Ge umbrella-flips into its preferred tetrahedral coordination.

Our results provide a clear explanation as to why switching in GST is fast and stable. This is because the crystallization–amorphization process does not require the rupture of strong covalent bonds and the transition is diffusionless. The facts that the Te sublattice is partially preserved as well as the conservation of the local structure around the Sb atoms, account for why the transformation can be easily reversed. The material does not have to be transformed into a truly liquid state. Bond rupture is believed to be due, at least partially, to electronic excitation. It also should be noted that the amorphous structure, at least on a local level, is well defined, enhancing the reversibility of the transition.

We would like to stress that it is a combination of different structural techniques that has allowed us to understand the structure of the crystalline phase of GST and its modification on amorphization. Although other structural models are possible (in the absence of more detailed bond angle information), we believe that the level of agreement between the EXAFS, XANES and XRD data provides strong support for the structural models we propose.

In another commercially used phase-change material, namely an AgInSbTe alloy, we have observed qualitatively similar behaviour, namely the first-nearest-neighbour peaks became stronger on amorphization. The binary GeTe also clearly exhibited a switch from tetrahedral to octahedral coordination on crystallization. We thus believe that the nature of the structural transformation discussed above is likely to be common for other phase-change media. The mechanism for the structural phase transition disclosed here provides potentially critical insight in the search for better performing materials for the next generation of faster and denser optical and Ovonic memories.

METHODS

EXAFS

EXAFS allows one to obtain information about the local structure around selected chemical species, such as the average coordination number, the bond lengths, the chemical nature of the neighbouring species, as well as the bond length disorder parameter, or mean-square relative displacement (MSRD). The technique is selective to the absorbing atom, which allows one to probe the local structure around different constituent elements independently.

X-ray absorption near-edge structure (XANES), which involves multiple scattering, additionally allows one to probe the local arrangement of atoms on a scale somewhat beyond the first-nearest neighbours, in particular, it is sensitive to the mutual arrangement of the neighbouring atoms in space, that is, includes bond-angle information. As XANES features are also a consequence of transitions from occupied core states to unoccupied conduction-band states, the spectra also contain information about the density of unoccupied conduction-band states. It should be mentioned that recent advances in theory, such as the development of the FEFF code, have made it possible to simulate EXAFS and XANES spectra with good accuracy[26].

To investigate the structure of crystallized GST and its modification on laser-pulse-induced amorphization, we have measured EXAFS and XANES spectra at the K-edges of all three constituent species. Measurements were performed in fluorescence mode for the Ge K-edge (at beamline BL12C at the Photon Factory, Tsukuba, Japan) and in conversion electron yield mode for the Sb and Te K-edges (at beamline BL01B1 at the SPring-8 synchrotron source, Japan). To achieve better statistics and maximum confidence in the results, the data obtained for the three edges were analysed concurrently.

SAMPLE PREPARATION

Our measurements were performed on real-device structures. A base substrate, a pre-grooved polycarbonate optical disc, of which the thickness and diameter were 0.6 mm and 120 mm, respectively, was used. A multilayer structure composed of ZnS–SiO_2 (130 nm)/GST (20 nm)/ZnS-SiO_2 (20 nm)/Al-alloy (100 nm) was successively deposited by radio-frequency magnetron sputtering at a pressure of 0.5 Pa. To transform the as-deposited amorphous GST layer into the crystalline state and laser-amorphized state, the sample disc was set and rotated on an optical disc drive tester (DDU-1000 with a 635-nm laser wavelength and 0.6 lens numerical aperture, Pulstec). First, the film was laser-crystallized twice continuously on both lands and grooves using a laser power of 6.0 mW and a constant linear velocity (CLV) of 2.0 m s^{-1}. Then, a pulsed-laser beam (12 mW at a frequency of 30 MHz) was focused on the film at a CLV of 12 m s^{-1} for re-amorphization. The amorphization level was confirmed by measuring the reflected beam intensity: the reflection was saturated at a much lower level than that of the fully crystallized layer but slightly higher than that of the as-deposited layer. Immediately before the measurements, the Al-alloy and the upper ZnS-SiO_2 layers were removed using Scotch tape, so that the uppermost layer was GST.

Received 25 December 2003; accepted 30 July 2004; published 12 September 2004.

References

1. Moller, S., Perlov, C., Jackson, W., Taussig, C. & Forrest, S. R. A polymer/semiconductor write-once read-many-times memory. *Nature* **426,** 161–169 (2003).
2. Ovshinsky, S. R. Reversible electrical switching phenomena in disordered structures. *Phys. Rev. Lett.* **21,** 1450–1453 (1968).
3. Ohta, T. Phase-change optical memory promotes the DVD optical disk. *J. Optoelectron. Adv. Mater.* **3,** 609–626 (2001).
4. Ohta, T. & Ovshinsky, S. R. in *Photo-induced Metastability in Amorphous Semiconductors* (ed. Kolobov, A. V.) 310–326 (Wiley-VCH, Berlin, 2003).
5. Petrov, I. I., Imamov, R. M. & Pinsker, Z. G. Electronographic determination of the structures of $Ge_2Sb_2Te_5$ and $GeSb_4Te_7$. *Sov. Phys. Crystallogr.* **13,** 339–344 (1968).
6. Gonzalez-Hernandez, J. *et al.* Free carrier absorption in the Ge:Sb:Te system. *Solid State. Commun.* **95,** 593–596 (1995).
7. Nonaka, T., Ohbayashi, G., Toriumi, Y., Mori, Y. & Hashimoto, H. Crystal structure of GeTe and $Ge_2Te_2Te_5$ meta-stable phase. *Thin Solid Films* **370,** 258–261 (2000).
8. Yamada, N. & Matsunaga, T. Structure of laser-crystallised $Ge_2Sb_{2+x}Te_5$ sputtered thin films for use in optical memory. *J. Appl. Phys.* **88,** 7020–7028 (2000).
9. Koningsberger, D. C. & Prins, R. (eds) *X-ray Absorption* (Wiley, New York, 1988).
10. Frenkel, A. I., Stern, E. A., Voronel, A., Qian, M. & Newville, M. Buckled crystalline structure of mixed ionic salts. *Phys. Rev. Lett.* **71,** 3485–3888 (1993).
11. Littlewood, P. B. The crystal structure of IV-VI compounds: 1. Classification and description. *J. Phys. C* **13,** 4855–4973 (1980).
12. Chattopadhyay, T., Boucherle, J. X. & von Schnering, H. G. Neutron diffraction study on the structural phase transition in GeTe. *J. Phys. C* **20,** 1431–1440 (1987).
13. Kolobov, A. V., Tominaga, J., Fons, P. & Uruga, T. Local structure of crystallized GeTe films. *Appl. Phys. Lett.* **82,** 382–384 (2003).
14. Privitera, S., Rimini, E., Bongiorno, C., Pirovano, A. & Bez, R. Crystallization and phase separation in $Ge_{2+x}Sb_2Te_5$ thin films. *J. Appl. Phys.* **94,** 4409–4413 (2003).
15. Vengalis, B. & Valatska, K. Phase segregaton in Te saturated GeTe. *Phys. Status Solidi B* **117,** 471–476 (1983).
16. Rabe, K. M. & Joannopoulos, J. D. Theory of the structural phase transition of GeTe. *Phys. Rev. B* **36,** 6631–6639 (1987).
17. Tominaga, J. *et al.* Ferroelectric catastrophe: beyond nanometer-scale optical resolution. *Nanotechnology* **15,** 411–415 (2004).
18. Wakagi, M., Ogata, K. & Nakano, A. Structural study of a-Si and a-Si:H films by EXAFS and Raman-scattering spectroscopy. *Phys. Rev. B* **50,** 10666–10671 (1994).
19. Njoroge, W. K., Woltgens, H. W. & Wuttig, M. Density changes upon crystallization of $Ge_2Sb_{2.04}Te_{4.74}$ films. *J. Vac. Sci. Technol. A* **20,** 230–233 (2002).
20. Brodsky, M. H. in *Light Scattering in Solids* (ed. Cardona, M.) 205–252 (Springer, Berlin, 1983).
21. Kalb, J., Spaepen, F. & Wuttig, M. Calorimetric measurements of phase transformations in thin films of amorphous Te alloys used for optical data storage. *J. Appl. Phys.* **93,** 2389–2393 (2003).
22. Yamada, N., Ohno, E., Nishiuchi, K., Akahira, N. & Takao, M. Rapid phase transitions of GeTe-Sb_2Te_3 pseudobinary amorphous thin films for optical disk memory. *J. Appl. Phys.* **69,** 2849–2856 (1991).
23. Ovshinsky, S. R. in *Insulating and Semiconducting Glasses* (ed. Boolchand, P.) 729–780 (World Scientific, Singapore, 2000).
24. Angell, C. A. in *Insulating and Semiconducting Glasses* (ed. Boolchand, P.) 1–52 (World Scientific, Singapore, 2000).
25. Yassievich, I. A. Recombination-induced defect heating and related phenomena. *Semicond. Sci. Technol.* **9,** 1933–1953 (1994).
26. Ankudinov, A. L., Ravel, B., Rehr, J. J. & Conradson, S. Real-space multiple-scattering calculation and interpretation of x-ray-absorption near-edge structure. *Phys. Rev. B* **58,** 7565–7576 (1998).

Acknowledgements

The XAFS measurements were performed at beamlines 12C at the Photon Factory, Japan, and BL01B1 at SPring-8, Japan as parts of proposals 2001G332 and 2001B0099-NX, respectively. A.V.K. would like to thank A. S. Mishchenko for a useful discussion. A. I. F. acknowledges support by the US Department of Energy Grant No. DE-FG02- 03ER15477.

Correspondence and requests for materials should be addressed to A.V.K.

Supplementary Information accompanies the paper on www.nature.com/naturematerials

Competing financial interests

The authors declare that they have no competing financial interests.